CHAPTER

Coursework Studies

15

15.1 Introduction

A number of coursework studies, or assignments, have been prepared for assessing the understanding and ability of graduate students to apply the material to protracted exercises. These are intended to reflect real-world practice. The five exercises included in this chapter are typical of the basic evaluations that are undertaken routinely in a professional flight dynamics environment and require the application of much of the material in this book. Further, since the aircraft models are of real aircraft the interested reader may easily expand the scope of the exercises by obtaining additional information and data from the source references. The exercises provide an opportunity for students to develop competence in the essential enabling skills relevant to the areas of flight control, flight dynamics, and flight test.

The notational style, theoretical background, and other information has been edited such that it is generally consistent with the material in this book, as far as that is possible. However, care should be taken with units, as both SI and American imperial units are used—again reflecting a relatively common situation in industry.

15.1.1 Working the assignments

Each assignment requires a mix of hand calculation, computational analysis, and graph plotting. Any convenient computational tools may be used, but they should be identified in the report. The use of MATLAB, Program CC, or similar is essential for these assignments; MS Excel may also be found useful for some data manipulation. Each assignment is structured as a set of tasks which should be undertaken sequentially to achieve satisfactory completion of the exercise. To provide experience in the solution process, the tasks are set out in the order in which they must be completed since, in most cases, each task builds on the output of the previous task. Clearly it is therefore most important that the solution process be undertaken in an orderly way and that the results of each task be assessed for correctness and validity before moving on to the next task.

15.1.2 Reporting

Plan and write a short report to summarise and present the results of each assignment and note that accurate presentation of results is important. For example, strip chart plots provide the most convenient illustration format for time history responses. Care should be exercised to show and explain the steps undertaken in working the assignment since the overall objective is to assess understanding, not the ability to simply process sequential calculations using tools like MATLAB or similar software. Supporting material and calculations may be included in appendices, but undocumented computer printout is generally unacceptable.

15.2 Assignment 1: Stability augmentation of the North American X-15 hypersonic research aeroplane

(CU 2011)

The North American X-15 (Heffley and Jewell, 1972) was a hypersonic research aeroplane which first flew in 1960. This rocket-powered aeroplane was capable of speeds as high as Mach 6 at up to 300,000 ft altitude. The aeroplane was carried under a B-52 to an altitude of about 45,000 ft, from which it was launched at a speed of about Mach 0.8. Following the powered phase of flight, recovery entailed gliding flight to a normal landing—much in the same way as the space shuttle recovery.

The first objective of the assignment is to review the stability and control properties of the aircraft for one typical flight condition. Since the aircraft was fitted with damping augmentation in each axis, the second objective is to design a simple damping augmentation control law for each control axis and to show the improvement in response thereby achieved.

15.2.1 The aircraft model

The aircraft equations of motion are given in the form of the decoupled state equations as follows. The flight condition assumed corresponds with Mach 2.0 at an altitude of 60,000 ft.

The longitudinal state equation is

$$\begin{bmatrix} \dot{u} \\ \dot{w} \\ \dot{q} \\ \dot{\theta} \end{bmatrix} = \begin{bmatrix} -0.00871 & -0.019 & -135 & -32.12 \\ -0.0117 & -0.311 & 1931 & -2.246 \\ 0.000471 & -0.00673 & -0.182 & 0 \\ 0 & 0 & 1 & 0 \end{bmatrix} \begin{bmatrix} u \\ w \\ q \\ \theta \end{bmatrix} + \begin{bmatrix} 6.24 \\ -89.2 \\ -9.80 \\ 0 \end{bmatrix} \delta_e$$

The lateral-directional state equation is

$$\begin{bmatrix} \dot{\beta} \\ \dot{p} \\ \dot{r} \\ \dot{\phi} \end{bmatrix} = \begin{bmatrix} -0.127 & 0.0698 & -0.998 & 0.01659 \\ -2.36 & -1.02 & 0.103 & 0 \\ 11.1 & -0.00735 & -0.196 & 0 \\ 0 & 1 & 0 & 0 \end{bmatrix} \begin{bmatrix} \beta \\ p \\ r \\ \phi \end{bmatrix} + \begin{bmatrix} -0.00498 & 0.0426 \\ 28.7 & 5.38 \\ 0.993 & -6.90 \\ 0 & 0 \end{bmatrix} \begin{bmatrix} \delta_a \\ \delta_r \end{bmatrix}$$

Velocities are given in ft/s, angular velocities in rad/s, and angles in rad ($g = 32.2$ ft/s^2).

15.2.2 The solution tasks

(1) Set up the longitudinal output equation to include the additional variables angle of attack α and flight path angle γ. Solve the longitudinal equations of motion and obtain a full set of properly annotated transfer functions.

(2) Review the longitudinal stability properties of the aeroplane and produce response time histories to best illustrate the longitudinal stability modes. Comment on the likely requirement for stability augmentation.

(3) Set up the lateral-directional output equation, solve the lateral-directional equations of motion, and obtain a full set of properly annotated transfer functions.

(4) Review the lateral-directional stability properties of the aeroplane and produce response time histories to best illustrate the lateral-directional stability modes. Comment on the likely requirement for stability augmentation.

(5) With the aid of an appropriate root locus plot for each control axis, design three simple damping augmentation control laws. Clearly state the design decisions and the expected change to the stability modes. The root locus plots should be annotated appropriately for this purpose.

(6) Augment the open-loop longitudinal state equation to include the control law, thereby creating the closed-loop state equation. Solve the closed-loop equations of motion and obtain a full set of properly annotated transfer functions.

(7) Augment the open-loop lateral-directional state equation to include the control laws, thereby creating the closed-loop state equation. Solve the closed-loop equations of motion and obtain a full set of properly annotated transfer functions.

(8) Compare the longitudinal closed-loop stability modes with those of the basic airframe and produce time histories to best illustrate the improvements to the response properties of the aeroplane.

(9) Compare the lateral-directional closed-loop stability modes with those of the basic airframe and produce time histories to best illustrate the improvements to the response properties of the aeroplane.

(10) Summarise the flight control system design and state the main changes seen in the augmented aeroplane. Draw simple block diagrams to illustrate the structure of the stability augmentation system.

15.3 Assignment 2: The stability and control characteristics of a civil transport aeroplane with relaxed longitudinal static stability

(CU 2001)(CU 2002)

The increasing use of fly-by-wire flight control systems in advanced civil transport aeroplanes has encouraged designers to consider seriously the advantages of relaxing the longitudinal controls-fixed static stability of the airframe. However, not all of the changes to the flying qualities of the aircraft with relaxed static stability (RSS) are beneficial, and some degree of design compromise is inevitable. The purpose of this assignment is to demonstrate by example typical changes to a conventional civil transport aeroplane following relaxation of its controls-fixed longitudinal stability margin. The implications for flight control system design are not considered.

15.3.1 The aircraft model

The Convair CV-880 was a 130-passenger, four-engined civil transport aeroplane which first flew in 1960. It was very similar in layout to most other jet transport aeroplanes of the time and had very benign stability and control characteristics. Flying controls were entirely mechanical and comprised servo tab deflected ailerons, elevator, and rudder, together with power operated spoilers for additional lateral-directional control. The aircraft does not appear to have been fitted with any kind of automatic stabilisation system. Data for this exercise was obtained, or derived, from that given by Heffley and Jewell (1972) and is reasonably accurate, as far as can be ascertained. The data should be read in the context of the longitudinal geometry of the CV-880 shown in Fig. 15.1. A typical level flight cruise condition has been selected for this exercise defined by the following parameters:

Free-stream Mach number	M_0	0.8	
Free-stream velocity	V_0	779	ft/s
Dynamic pressure	$Q = \frac{1}{2}\rho V_0^2$	224	Lb/ft^2
Altitude	h	35,000	ft
Air density	ρ	0.000738	slug/ft^3
Body trim incidence	α_e	4.7	deg

Aircraft geometric, weight, and *cg* information are given as follows:

Weight	W	155,000	Lb
Mass	m	4814	slug
Moment of inertia in pitch	I_y	251,0000	slugft^2
Mean geometric chord (*mgc*)	$\overline{c}$	18.94	ft
Wing area	S_w	2000	ft^2
Wing span	b	120	ft
Tailplane area	S_T	400	ft^2
Tail moment arm	l_T	57	ft
Tailplane trim angle	η_T	−3.0	deg
cg position (referenced to *mgc*)	h	0.25	
Wing-body aerodynamic centre position (referenced to *mgc*)	h_0	0.09	
Thrust line inclination wrt HFD	i	3	deg
Thrust moment arm about *cg*	l_{tr}	2	ft

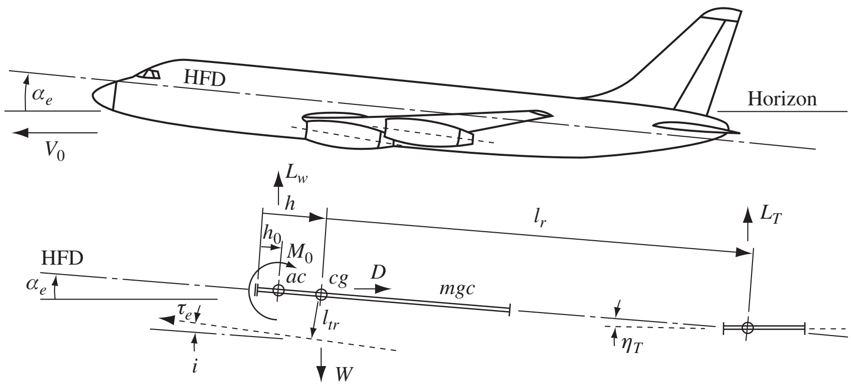

FIGURE 15.1 Longitudinal geometry of the Convair CV-880.

Note that the reference chord given is the mean geometric chord (*mgc*) rather than the more usual mean aerodynamic chord (*mac*), and it may be used in the same way in the calculations. The aircraft is fitted with an all-moving tailplane for trim, and its trim angle is equivalent to the tailplane setting angle of a fixed tailplane. The longitudinal geometric reference is the horizontal fuselage datum (HFD).

Relevant aerodynamic characteristics at the operating flight condition are as follows:

Total drag coefficient	C_D	0.024	
Wing-body aerodynamic pitching moment coefficient	C_{m_0}	−0.1	
Wing lift curve slope	a	4.8	rad^{-1}
Tailplane lift curve slope	a_1	3.75	rad^{-1}
Elevator lift curve slope	a_2	0.95	rad^{-1}
Wing downwash at tail	$d\varepsilon/d\alpha$	0.37	

The dimensionless longitudinal aerodynamic stability and control derivatives referred to aircraft wind axes for the flight condition of interest are given as follows:

X_u	−0.0485	Z_q	−3.7091
Z_u	−0.6978	$M_{\dot{w}}$	−2.2387
M_u	−0.0055	M_q	−5.9983
X_w	0.1920		
Z_w	−4.8210	X_η	−0.0001
M_w	−0.6492	Z_η	−0.1456
$Z_{\dot{w}}$	−1.3543	M_η	−0.4408

15.3.2 The governing trim equations

Lift forces: $L_{total} = L_w + L_T + \tau \sin(i + \alpha_e) = W$

Drag forces: $D = \tau \cos(i + \alpha_e)$

Pitching moment about *cg*: $M = M_0 + L_w(h - h_0)\bar{c}\cos\alpha_e + D(h - h_0)\bar{c}\sin\alpha_e + \tau l_{tr} - L_T l_T$

Tailplane lift coefficient, assuming a symmetric aerofoil section: $C_{L_T} = a_1(\alpha_T + \eta_T) + a_2\eta$

Tailplane angle of attack: $\alpha_T = \frac{C_{L_w}}{a}\left(1 - \dfrac{d\varepsilon}{d\alpha}\right)$

15.3.3 Basic aircraft stability and control analysis

Working with the equations in coefficient form, obtain values for the following:

Trim wing-body lift coefficient: C_{L_w}
Trim tailplane lift coefficient: C_{L_T}
Trim elevator angle: η
Controls-fixed neutral point: h_n
Controls-fixed static margin: K_n

What tailplane trim angle η_T would be required to enable the elevator trim angle to be set at zero?

Set up and solve the equations of motion referred to wind axes and obtain values for the stability modes characteristics. By applying the final value theorem to each of the control transfer functions, assuming a unit step input, obtain estimates for the steady-state control sensitivity of the aircraft.

15.3.4 Relaxing the stability of the aircraft

The longitudinal static stability of the aircraft is now relaxed by shifting the *cg* aft by 12% of the *mgc*. In practice this would also be accompanied by design changes to the aerodynamic configuration of the aircraft, especially of the tail geometry. However, for the purpose of this exercise, the aerodynamic properties of the aeroplane are assumed to remain unchanged.

Clearly, this change will modify the trim state and it will also modify those aerodynamic stability and control derivatives which have a dependency on tail volume ratio and tail moment arm. Calculate a new value for tail volume ratio and tail moment arm, and calculate new values for those derivatives affected by the aft shift in *cg* position.

15.3.5 Relaxed stability aircraft stability and control analysis

Repeat the computational stability and control exercise for the relaxed-stability aircraft to obtain new values for all of the variables defining the stability and control characteristics at the same flight condition.

15.3.6 Evaluation of results

Tabulate the results of the analyses to facilitate comparison of the unmodified aircraft stability and control characteristics with those of the relaxed-stability aircraft. Summarise the observations with particular reference to the advantages and disadvantages of relaxing the stability of a civil transport aircraft. Comment also on the obvious limitations of this exercise and the validity of the estimated variable changes.

15.3.7 Postscript

Do not expect to see dramatic changes in the stability and control characteristics of the aircraft following relaxation of stability by shifting the *cg* aft.

15.4 Assignment 3: Lateral-directional handling qualities design for the Lockheed F-104 Starfighter aircraft

(CU 2011)

The lateral-directional flying qualities of the Lockheed F-104 aircraft are typical of many high-performance aircraft. The airframe is not very stable, and its stability and control characteristics vary considerably with flight condition. Consequently, it is necessary to augment the stability and control characteristics by means of a flight control system. Since the airframe properties vary with flight condition, it is necessary to vary, or schedule, the control system gains with flight condition in order to achieve reasonably even handling qualities over the flight envelope.

The objective of the assignment is to evaluate the lateral-directional stability and control characteristics of the F-104 at three representative Mach numbers at sea level only. With an understanding of the basic unaugmented airframe, the task is then to design a simple command and stability augmentation system to give the aircraft acceptable roll handling characteristics over the Mach number range. This will require proposing suitably simple schedules for the flight control system gains.

15.4.1 The aircraft model

The Lockheed F-104 Starfighter aircraft is a small single-engined combat aircraft which first flew in the mid-1950s. The aircraft was supplied to many air forces around the world and remained in service well into the 1970s, and during its service life many variants were developed. The aircraft configuration is typical of the time: a long slender fuselage, low-aspect-ratio unswept wing, and a T tail mounted on a relatively small fin. The airframe is nominally stable at all flight conditions, although the degree of stability is generally unacceptably low. The flying controls are entirely mechanical with a simple three-axis stability augmentation system. The aircraft is capable of a little over Mach 1.0 at sea level and as much as Mach 2.0 at high altitude. Data for this exercise were obtained from Heffley and Jewell (1972) and is reasonably accurate, as far as is known.

Note that American imperial units are implied throughout and should be retained in this work. The American sign convention for aileron and rudder control is the reverse of that defined in this book.

The Laplace transform of the lateral-directional equations of motion, referred to a body axis system, is given in the following format:

$$\begin{bmatrix} 1-y_v & -\dfrac{W_e s + g\cos\theta_e}{V_e} & \dfrac{U_e s - g\sin\theta_e}{V_e s} \\ -l_\beta & s(s-l_p) & -l_r \\ -n_\beta & -n_p s & s-n_r \end{bmatrix} \begin{bmatrix} \beta(s) \\ p(s)/s \\ r(s) \end{bmatrix} = \begin{bmatrix} y_\xi & y_\zeta \\ l_\xi & l_\zeta \\ n_\xi & n_\zeta \end{bmatrix} \begin{bmatrix} \xi(s) \\ \zeta(s) \end{bmatrix}$$

with auxiliary equations

$$\begin{aligned} v(s) &= V_e \beta(s) \\ \phi(s) &= \frac{p(s)}{s} + \frac{r(s)}{s}\tan\theta_e \\ \psi(s) &= \frac{1}{\cos\theta_e}\frac{r(s)}{s} \end{aligned}$$

Note that the derivatives are concise derivatives; they have dimensions and are equivalent to the usual dimensional derivatives divided by mass or inertia terms as appropriate.

Numerical data for the three sea-level flight conditions are given in the following table.

Aerodynamic Data for the Lockheed F-104A Starfighter Aircraft					
Flight Condition	**#**		**1**	**2**	**3**
Trim Data					
Altitude	h	ft	0	0	0
Air density	ρ_0	slug/ft^3	0.00238	0.00238	0.00238
Speed of sound	a_0	ft/s	1116.44	1116.44	1116.44
Gravitational constant	g	ft/s^2	32.2	32.2	32.2
Trim Mach number	M_e		0.257	0.800	1.100
Trim attitude	θ_e	deg	2.30	2.00	1.00
Concise Derivative Data					
y_v		1/s	−0.178	−0.452	−0.791
l_β		1/s^2	−20.9	−146.0	−363.0
n_β		1/s^2	2.68	13.60	42.70
l_p		1/s	−1.38	−4.64	−7.12
n_p		1/s	−0.0993	−0.188	−0.341
l_r		1/s	1.16	3.67	7.17
n_r		1/s	−0.157	−0.498	−1.060
y_ξ		1/s	0	0	0
l_ξ		1/s^2	4.76	49.6	81.5
n_ξ		1/s^2	0.266	3.510	6.500
y_ζ		1/s	0.0317	0.0719	0.0621
l_ζ		1/s^2	5.35	41.50	57.60
n_ζ		1/s^2	−0.923	−7.070	−8.720

15.4.2 Lateral-directional autostabiliser structure

A typical lateral-directional autostabiliser structure is shown in Fig. 15.2 and is quite representative of the system fitted to the F-104. Note that it is simplified by removing sensor dynamics, artificial feel system dynamics, surface actuator dynamics, and various feedback signal filtering. The feedback gains K_p and K_r are chosen to augment the lateral-directional stability modes to acceptable levels of stability. The washout filter time constant T_w is chosen to give the aircraft acceptable steady turning performance. The *aileron-rudder interlink* gain K_{ari} is chosen to minimise adverse sideslip during the turn entry.

15.4.3 Basic aircraft stability and control analysis

(1) Derive the open-loop aircraft state equation, which should have the following form:

$$\dot{\mathbf{x}}(t) = \mathbf{A}\mathbf{x}(t) + \mathbf{B}\mathbf{u}(t)$$

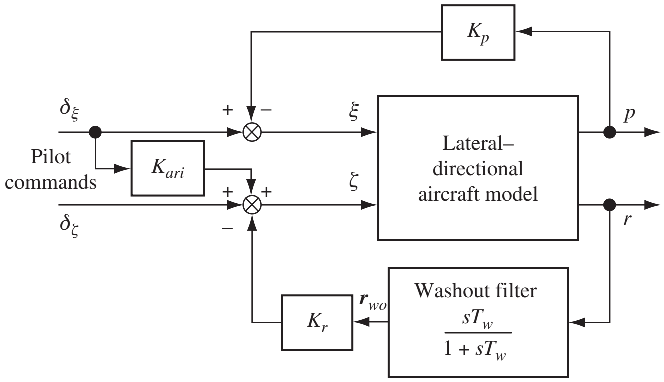

FIGURE 15.2 Simplified lateral-directional autostabiliser.

where the state vector

$$\mathbf{x}(t)^{\mathrm{T}} = \begin{bmatrix} \beta(t) & p(t) & r(t) & \phi(t) \end{bmatrix}$$

and the input vector

$$\mathbf{u}(t)^{\mathrm{T}} = \begin{bmatrix} \xi(t) & \zeta(t) \end{bmatrix}.$$

State clearly any assumptions made.

(2) Obtain the response transfer functions from the solution of the state equation for the three flight conditions for which data are provided. Show the transfer functions in factorised form.

(3) Obtain time history plots showing the response to a short pulse of aileron and a short pulse of rudder. The plots should be presented in strip chart form showing all four variables for a period of 10 seconds. The pulse lengths should be chosen to emphasize the dynamics of turn entry.

(4) Comment on the stability modes characteristics and their variation over the flight envelope of interest, and identify any deficiencies needing improvement. Comment also on the turn performance of the aircraft and suggest how this might be improved. Remember that the pilot commands a turn using the aileron and only uses the rudder to "tidy" the turn entry.

15.4.4 Augmenting the stability of the aircraft

(5) With the aid of the appropriate root locus plots, investigate the feedback gains, K_p and K_r, required to improve the stability modes characteristics for all three flight conditions. Ignore the washout filter at this stage. Aim to achieve the following closed-loop mode characteristics: roll mode time constant of less than one second, a stable spiral mode, and dutch roll damping $0.5 > \zeta_d > 0.3$. Explain why a roll rate feedback gain $K_p = 0$ is a good solution for the lateral axis at all three flight conditions.

(6) It is typical to schedule feedback gains with dynamic pressure ($Q = \frac{1}{2}\rho V_0^2$), as shown in Fig. 15.3. Plot out the upper and lower limits of the values of K_r that meet the stability requirements for each flight condition as a function of Q. Hence design a gain schedule like that shown in Fig. 15.3. State the value of K_r for each flight condition according to your schedule and confirm that the values are consistent with your analysis of tasks (3) and (4). These are the values that you should use in your subsequent work.

(7) With reference to Fig. 15.2, the autostabiliser control law may be written as

$$\mathbf{u}(t) = \mathbf{L}\mathbf{u}_1(t) - \mathbf{K}\mathbf{x}(t)$$

where

$$\mathbf{u}_1(t)^{\mathrm{T}} = \begin{bmatrix} \delta_\xi & \delta_\zeta \end{bmatrix}$$

is the vector of pilot commands,

$$\mathbf{L} = \begin{bmatrix} 1 & 0 \\ K_{ari} & 1 \end{bmatrix}$$

is the input mixing matrix, and $\mathbf{K}$ is the matrix of feedback gains. Omitting the aileron-rudder interlink for the moment, $K_{ari} = 0$, write down the matrices $\mathbf{K}$ and $\mathbf{L}$ and calculate the closed-loop state equation for all three flight conditions,

$$\dot{\mathbf{x}}(t) = \mathbf{A}\mathbf{x}(t) + \mathbf{B}\mathbf{u}_1(t)$$

where now, of course, the matrices $\mathbf{A}$ and $\mathbf{B}$ are the closed-loop versions.

(8) Obtain the response transfer functions from the solution of the closed-loop state equation developed in (7) for the three flight conditions for which data is provided. Show the transfer functions in factorised form.

(9) Obtain time history plots showing the response to a short pulse of aileron and a short pulse of rudder. Again, the plots should be presented in strip chart form showing all four variables for a period of 10 seconds. The object here is to show and confirm the improvement in the basic airframe dynamics; the time histories also provide a "baseline" with which to compare the responses developed in the following sections.

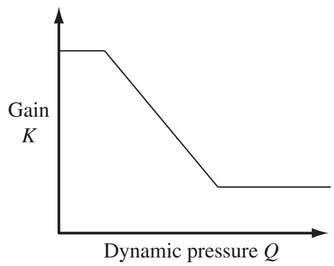

FIGURE 15.3 Typical gain schedule.

15.4.5 Inclusion of the washout filter in the model

(10) Modify the open-loop aircraft state equation derived in (1) to include the additional state variable r_{wo} introduced by the filter, so that the state vector becomes

$$\mathbf{x}(t)^{\mathrm{T}} = \begin{bmatrix} \beta(t) & p(t) & r(t) & \phi(t) & r_{wo}(t) \end{bmatrix}.$$

Set the washout filter time constant to the typical value of one second, $T_w = 1.0$ s. Obtain the open-loop state equation for each of the three flight conditions.

(11) Modify the control law derived in (7) to include the additional washout filter state variable and calculate the closed-loop state equation for the three flight conditions. Take care to re-define the feedback matrix **K** correctly and set the aileron-rudder interlink gain to zero as before.

(12) Obtain the revised closed-loop response transfer functions for the three flight conditions and show the transfer functions in factorised form. What does the addition of the washout filter do to the closed-loop stability modes of the aircraft?

(13) Obtain time history plots showing the response to a short pulse of aileron and a short pulse of rudder. Compare the responses with those obtained in (9) by plotting both sets of time histories on the same axes; once again, the plots should be presented in strip chart form showing the four aircraft motion variables only.

(14) Identify the differences in the plots and hence explain the purpose of the washout filter. Remember that the object is to review turning performance in response to aileron command. Comment also on the initial transient in sideslip angle.

15.4.6 Designing the aileron-rudder interlink gain

(15) The objective here is to design a suitable value for the interlink gain K_{ari} for each of the three flight conditions. In the present context this may be done only by choosing a test value and including it in the input mixing matrix **L** in the closed-loop model developed in (11), obtaining the transfer functions, and observing the response to an aileron command. The correct value of K_{ari} is the minimum value that will cancel the adverse sideslip response seen in the transient immediately following application of the aileron command. Suitable values of gain lie in the range $0 < K_{ari} < 0.5$. Define a simple gain schedule as a function of dynamic pressure Q.

(16) Write down the fully developed closed-loop state equations for all three flight conditions, including the aileron-rudder interlink gain according to the schedule designed in (15).

(17) Obtain and show in factorised form the response transfer functions for all three flight conditions. Note any changes due to the inclusion of the aileron-rudder interlink gain.

(18) Demonstrate the turning performance of the F-104 with the fully developed control law by showing the response to an aileron pulse. As before, the response of all four motion variables should be shown in strip chart format.

(19) Identify the key attributes of the turning performance as refined by the control law design. In particular explain the response changes due to the aileron-rudder interlink. This will be easier to do if a comparison is made with the responses obtained in (8).

15.5 Assignment 4: Analysis of the effects of Mach number on the longitudinal stability and control characteristics of the LTV A7-A Corsair aircraft

(CU 2003)

The object of the assignment is to analyse, illustrate, and explain the effects of compressibility on the longitudinal aerodynamics, stability, and control of a typical 1960s combat aeroplane.

15.5.1 The aircraft model

The aircraft chosen for this exercise is the Ling-Tempco-Vought (LTV) A7-A Corsair, a carrier-based aircraft which first flew in the mid-1960s. The aircraft is typical for its time: a single pilot, single engine aircraft built to withstand the rigours of operating from a carrier deck. The airframe is nominally stable at all flight conditions, although the degree of stability is generally unacceptably low. Consequently, the aircraft is fitted with a simple three-axis stability augmentation system. The aircraft is capable of speeds up to approximately Mach 1.2, and four data sets covering the full Mach number range at an altitude of 15,000 ft are given in Teper (1969). The data for this exercise were obtained directly, or derived, from the data given in Teper; it is listed in Table 15.1 and has been adjusted to a consistent set of units, with the exception of altitude, which is retained in ft units. Be aware that some variables are given for information only and are not required in the calculations.

The aerodynamic data are referenced to an aircraft wind axis system.

15.5.2 The assignment tasks

All assumptions made should be very clearly stated.

Assembling the derivatives

Using simple mathematical approximations for the longitudinal stability and control derivatives together with the data given in Table 15.1, calculate values for the dimensionless derivatives and the static and manoeuvre stability parameters; hence complete Table 15.2 for all four flight conditions. Note that the usual tailplane approximation for the derivatives M_q, M_η, and Z_η is not assumed. These derivatives should be calculated from first principles, for example, in the same way as M_u and Z_w.

Solving the equations of motion

Writing the longitudinal state equation as $\mathbf{M}\dot{\mathbf{x}} = \mathbf{A}'\mathbf{x} + \mathbf{B}'\mathbf{u}$, write down the matrices $\mathbf{M}$, $\mathbf{A}'$, and $\mathbf{B}'$ in algebraic form, stating the elements in terms of dimensionless derivatives. In the interests of simplicity, the equations of motion should be referred to aircraft wind axes. Hence, obtain the aircraft response transfer functions for each of the four flight conditions.

Assessing the dynamic stability characteristics

Tabulate the closed-loop longitudinal stability modes characteristics for each of the four flight conditions. Produce response time histories which best show the stability modes dynamics for the unaugmented aircraft for all flight conditions. Assess the stability modes against the requirements for Level 1 flying qualities.

Table 15.1 LTV A-7A Corsair Aerodynamic, Geometric, and Flight Condition Data

Flight Case #		1	2	3	4
Altitude	h (ft)	15000	15000	15000	15000
Mach number	M_0	0.3	0.6	0.9	1.1
Air density	ρ (kg/m^3)	0.7708	0.7708	0.7708	0.7708
Velocity	V_0 (m/s)	96.6	193.6	290.2	354.8
Trim body incidence	α_e (deg)	13.3	4.0	2.5	2.9
Trim elevator angle	η_e (deg)	−8.80	−3.80	−3.85	−4.95
Trim lift coefficient	C_L	0.420	0.200	0.095	0.030
Trim drag coefficient	C_D	0.036	0.018	0.020	0.054
	$\partial C_L/\partial\alpha$ (1/rad)	3.90	4.35	5.35	4.80
	$\partial C_D/\partial\alpha$ (1/rad)	1.20	0.30	0.23	0.22
	$\partial C_m/\partial\alpha$ (1/rad)	−0.48	−0.44	−0.59	−1.08
	$\partial C_m/\partial q$ (1/rad/s)	−0.0664	−0.0337	−0.0231	−0.0188
	$\partial C_L/\partial M$	0.030	0.012	0.058	0.047
	$\partial C_D/\partial M$	0.054	0	0.090	−0.013
	$\partial C_m/\partial M$	0	0.0010	−0.0360	−0.0055
	$\partial C_L/\partial\eta$ (1/rad)	0.585	0.600	0.550	0.400
	$\partial C_m/\partial\eta$ (1/rad)	−0.89	−0.91	−0.89	−0.63
	$d\varepsilon/d\alpha$	0.179	0.202	0.246	−0.247
Mass	m (kg)	9924	9924	9924	9924
Pitch inertia	I_y (kgm^2)	79946	79946	79946	79946
cg position	h	0.3	0.3	0.3	0.3
Wing area	S (m^2)	34.84	34.84	34.84	34.84
Mean chord	$\bar{\bar{c}}$ (m)	3.29	3.29	3.29	3.29
Tail moment arm	l_T (m)	5.5	5.5	5.5	5.5

Stability augmentation

Assuming a simple pitch damping stability augmentation system and, with the aid of root locus plots, design values for pitch rate feedback gain K_q in order to achieve a short-period mode damping ratio of about $0.5 \sim 0.7$ for each of the four flight conditions. Calculate the closed-loop state equations and hence obtain the response transfer functions for the augmented aircraft. Tabulate the closed-loop longitudinal stability modes characteristics for each of the four flight conditions. Produce response time histories which best show the stability modes dynamics for the augmented aircraft. It is most helpful if the response time histories for the previous tasks are plotted on the same axes for comparison purposes.

Assessing the effects of Mach number

Plot the following parameters against Mach number: C_L, C_D, α_e, η_e, K_n, H_m, Z_η, M_η, and K_q. Plot also the stability modes change with Mach number for both the unaugmented and augmented aircraft on the s-plane. Discuss and explain briefly the effect of Mach number on the following:

Table 15.2 LTV A-7A Corsair Aerodynamic Stability and Control Summary

Flight Case #		**1**	**2**	**3**	**4**
Altitude	h (ft)	15000	15000	15000	15000
Mach number	M_0	0.3	0.6	0.9	1.1
Air density	ρ (kg/m^3)	0.7708	0.7708	0.7708	0.7708
Velocity	V_0 (m/s)	96.6	193.6	290.2	354.8
Trim body incidence	α_e (deg)	13.3	4.0	2.5	2.9
Trim elevator angle	η_e (deg)	−8.80	−3.80	−3.85	−4.95
Trim lift coefficient	C_L	0.420	0.200	0.095	0.030
Trim drag coefficient	C_D	0.036	0.018	0.020	0.054
Dimensionless Aerodynamic Stability and Control Derivatives Referred to Wind Axes					
	X_u				
	X_w				
	X_q	0	0	0	0
	$X_{\dot{w}}$	0	0	0	0
	Z_u				
	Z_w				
	Z_q				
	$Z_{\dot{w}}$				
	M_u				
	M_w				
	M_q				
	$M_{\dot{w}}$				
	X_η	0	0	0	0
	Z_η				
	M_η				
Aircraft Geometric, Mass, and Inertia Data					
Mass	m (kg)	9924	9924	9924	9924
Pitch inertia	I_y (kg.m^2)	79946	79946	79946	79946
Wing area	S (m^2)	34.84	34.84	34.84	34.84
Mean chord	$\bar{\bar{c}}$ (m)	3.29	3.29	3.29	3.29
Tail moment arm	l_T (m)	5.5	5.5	5.5	5.5
Aircraft Stability and Control Parameters					
cg position	h	0.3	0.3	0.3	0.3
Static margin—controls-fixed	K_n				
Neutral point—controls-fixed	h_n				
Longitudinal relative density factor	μ_1				
Manoeuvre margin—controls-fixed	H_m				
Manoeuvre point—controls-fixed	h_m				

- Static stability and trim
- Dynamic stability and response
- Elevator control characteristics
- Feedback gain schedule

15.6 Assignment 5: The design of a longitudinal primary flight control system for an advanced-technology UAV

All assumptions made should be very clearly stated.

The object of the study is to design a representative longitudinal *primary flight control system* (PFCS) for an advanced technology UAV. The purpose of the PFCS is to provide a stable controllable aircraft platform with provision for pitch attitude command and speed command inputs. Typically, control commands originate from an automatic guidance and control system, or from a remote manual control station. Since the aircraft is pilotless, the application of handling qualities design criteria is not appropriate. However, the design of the PFCS should anticipate and reflect performance characteristics compatible with the aircraft role. Conventional aircraft flying qualities requirements may provide appropriate guidance in this context, although strict adherence to performance limits determined for piloted aircraft is not necessary.

15.6.1 The aircraft model

The Demon aircraft, shown in Fig. 15.4, is a small advanced-technology research UAV, developed by BAE Systems in conjunction with a number of UK universities over a period of several years, and culminating in a first flight late in 2010. The FLAVIIR (Buonanno, 2009) programme was jointly funded by BAE Systems and the UK Engineering and Physical Sciences Research Council. The School of Engineering at Cranfield University performed the lead design role for the project.

The Demon was developed to demonstrate a number of advanced technologies—in particular, to demonstrate the application of flapless flight control in which conventional flap control surfaces are replaced with circulation control devices. This was found to provide a significant design

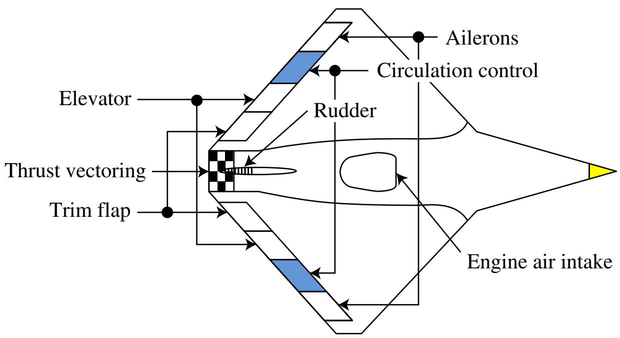

FIGURE 15.4 Demon UAV plan view.

challenge, and early flights of the vehicle were made with a mix of conventional and fluidic controls. The fluidic controls are indicated in the trailing edge of the wing in Fig. 15.4. The Demon has a take-off mass of approximately 44 kg, a wing span of 2.2 m, and a maximum speed of about 100 knots. Propulsive power is provided by a small gas turbine the exhaust of which is vectored in pitch by blown fluidic control means. Since the blown controls require high flow rates of high-pressure air, this is provided by a secondary gas turbine mounted in the nose of the vehicle. The flight control system of the vehicle is configured to allow both remote manual and fully autonomous control using various combinations of conventional and blown effectors. Initial flights have been made using remote manual control only.

In order to create simulation models of the Demon, aerodynamic and other data were developed using theoretical and empirical methods, and by static and dynamic wind tunnel testing at reduced scale. A description of some aspects of this work may be found in Buonanno (2009), and the linearised equations of motion were obtained from the simulation model developed by Saban (2006). The equations of motion relate to an early representation of the Demon and are known to be of doubtful accuracy in some aspects of the aerodynamic description. However, the equations of motion are sufficient for the present purpose and have been adjusted to ensure consistency of units.

The longitudinal equations of motion corresponding with a flight speed of 45 m/s m/s at an altitude of 1000 m are given in *concise* state form:

$$\dot{\mathbf{x}} = \mathbf{A}\mathbf{x} + \mathbf{B}\mathbf{u}$$

where

$$\mathbf{x}^{\mathrm{T}} = \begin{bmatrix} u & w & q & \theta \end{bmatrix} \quad \mathbf{u}^{\mathrm{T}} = \begin{bmatrix} \eta & \tau \end{bmatrix}$$

$$\mathbf{A} = \begin{bmatrix} -0.0324 & 0.137 & -2.2382 & -9.7972 \\ -0.252 & -3.7906 & 44.4781 & -0.5006 \\ 0.0291 & -0.7668 & -0.2658 & -0.132 \\ 0 & 0 & 1 & 0 \end{bmatrix} \quad \mathbf{B} = \begin{bmatrix} 0.4126 & 2.5267 \\ -22.1866 & 0 \\ -37.99 & -0.1134 \\ 0 & 0 \end{bmatrix}$$

The variables u, w have units m/s, q has units rad/s, θ and η have units rad, and thrust τ has units N.

The engine control lag has a time constant $T_\tau = 0.334$ s and is given by the transfer function

$$\frac{\tau(s)}{\tau_d(s)} = \frac{1}{(1 + 0.334s)}$$

with corresponding time domain equation $\dot{\tau} = -2.994\tau + 2.994\tau_d$.

The "elevator" control actuator is a typical model aircraft control servo and is represented by the second order transfer function

$$\frac{\eta(s)}{\eta_d(s)} = \frac{625}{(s^2 + 30s + 625)}$$

with corresponding state equation

$$\begin{bmatrix} \dot{\eta} \\ \dot{v}_\eta \end{bmatrix} = \begin{bmatrix} 0 & 1 \\ -625 & -30 \end{bmatrix} \begin{bmatrix} \eta \\ v_n \end{bmatrix} + \begin{bmatrix} 0 \\ 625 \end{bmatrix} \eta_d$$

15.6.2 The design requirements

A typical structure for the PFCS is shown in Fig. 15.5, in which longitudinal control of the aircraft is effected by independent control of speed, or thrust, and pitch attitude.

The requirement is to design appropriate values for the system gains and command path filters to give the controlled aircraft flying qualities compatible with the flight dynamics of the airframe. Common standard flying qualities requirements are not generally available for UAVs, so it is useful, but not essential, to refer to piloted aircraft requirements for guidance. It is probably prudent to seek higher levels of stability in a UAV, but it must be remembered that higher system gains will demand a higher power-bandwidth capability of the FCS and an acceptable design compromise must be found. The design should seek to achieve the following;

- Good step response characteristics: 1:1 relationship between steady-state command and response—little or no overshoot; short settling time—no intrusive lag effects.
- A closed-loop engine lag time constant that must not be allowed to become too long.
- Closed-loop elevator actuator properties that must not be allowed to diverge too far from their open-loop properties.
- Avoidance of closed-loop thrust and elevator demand saturation during normal operation.
- Avoidance of intrusive oscillatory response characteristics.
- Optional command path filtering that may be used for closed-loop response shaping.

The following points offer some guidance on the solution of the assignment.

- It is important to appreciate the flight dynamics characteristics of the basic airframe and to maintain close attention to the changes in the characteristics at each step of the design process. It is not good design practice to seek system performance beyond the capabilities of the airframe, engine, and actuator.
- The closure of three feedback loops will cause favourable and unfavourable interactions on the overall system performance. It is essential to understand the effects of each loop closure (guidance may be found in Chapter 11).

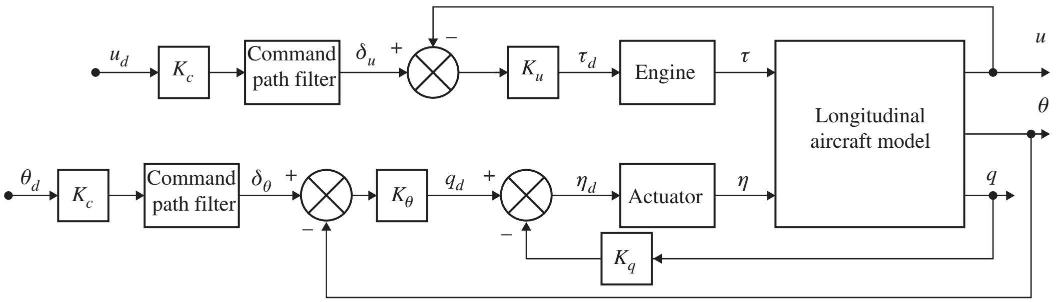

FIGURE 15.5 Typical PFCS controller architecture.

- Both controlled variables are dominant in phugoid dynamics, and control loop interactions may be expected. It is preferable, but not necessary, to design the speed control loop first to fix the closed-loop phugoid dynamics as desired. The pitch control loops are then more easily designed with the speed control loop closed.
- Trial and error solutions using tools such as Simulink are not acceptable. Do not be tempted to repeat each design step many times in an effort to achieve a "good" result. It is far better to produce a carefully explained coherent PFCS solution, even if its performance is not perfect. However, some limited trial and error investigations will be necessary in order to properly appreciate the interactions between control loops.

15.6.3 The assignment tasks

Solving the equations of motion

Solve the two input state equation and write out all eight of the response transfer functions. Evaluate the stability characteristics of the aircraft and the steady gain of each of the transfer functions. Decide on the desired stability properties of the aircraft with PFCS; justify and explain your choices. Review and comment on the control sensitivity of the aircraft with respect to the response variables of interest.

Designing the speed control loop

To facilitate the design of the speed controller, simplify the open-loop state equation to include the single thrust control input only. Augment the state equation to include the engine dynamics. With the aid of a properly annotated root locus plot, assess the effect of the feedback gain K_u on the closed-loop stability characteristics of the controller. State and justify your choice of feedback gain value. Calculate the closed-loop state equation, and solve and list the closed-loop transfer functions. Comment on the closed-loop stability properties and the steady-state gains of the transfer functions.

Assessing the performance of the speed controller

Using the closed-loop transfer function u/δ_u, describe and assess the unit step response. Explain the response shape and, if appropriate, design a first-order command path filter to refine the response shape. Adjust the command path gain K_c to obtain $u/u_d = 1.0$ in the steady state. Show a unit step response for the aircraft with your completed speed controller and comment on its ability to meet the general design requirements.

Re-arranging the system state model with speed loop closed

To design the pitch controller, it is first necessary to rearrange the model, with the speed control loop closed, and to enable the single elevator input only. Using the state equation with speed feedback loop closed, replace the thrust/speed input terms with the elevator input terms from the open-loop model equations of motion. Augment the state equation to include the elevator actuator model—the state equation should now be seventh-order. Solve the resulting state equation and write out all seven transfer functions. Identify and evaluate all of the stability modes and the steady gain of each of the transfer functions. Decide on your strategy for designing the pitch controller, and justify and explain your approach.

Designing the pitch rate control loop

With the aid of a properly annotated root locus plot using the transfer function q/η_d from the previous task, assess the effect of feedback gain K_q on the closed-loop stability characteristics. Similarly, construct a root locus plot using the transfer function θ/η_d from the previous task and assess the effect of feedback gain K_θ on the closed-loop stability characteristics. In the context of the design requirements, compare the effects of these assessments and hence decide on a suitable value for K_q. Calculate the closed-loop state equation by closing the pitch rate q feedback loop using your designed value of K_q. Solve the new closed-loop state equation and list all seven response transfer functions.

Designing the pitch attitude control loop

Finally, to complete the design of the pitch attitude control loop, create a root locus plot using the response transfer function θ/q_d from the previous task. Choose a suitable value for K_θ, paying particular attention to the closed-loop stability modes, engine lag, and elevator actuator characteristics. Calculate the closed-loop state equation with both q and θ loops closed using your designed gain values. Solve and obtain the closed-loop response transfer functions. Comment on the closed-loop stability properties and the steady-state gains of the transfer functions.

Assessing the performance of the pitch attitude controller

Using the closed-loop transfer function θ/δ_θ, describe and assess the unit step response. Explain the response shape and, if appropriate, design a first-order command path filter to refine the response shape. Adjust the command path gain K_c to obtain $\theta/\theta_d = 1.0$ in the steady state. Show a unit step response for the aircraft with your completed pitch attitude controller and comment on its ability to meet the general design requirements.

References

Buonanno, A. (2009). *Aerodynamic circulation control for flapless flight control of an unmanned air vehicle.* Cranfield, Bedfordshire: Cranfield University, PhD diss.

Flapless Aerial Vehicle Integrated Interdisciplinary Research programme (FLAVIIR). (2004) <www.flaviir.com>. (Numerous additional information sources and photographic images can also be found on the Internet.)

Heffley, R. K., & Jewell, W. F. (1972). *Aircraft handling qualities data.* Washington, DC: National Aeronautics and Space Administration, NASA Contractor Report NASA CR-2144.

Saban, D. (2006). *Flight control system design for the "demon" vehicle.* Cranfield, Bedfordshire: Cranfield University, MSc thesis.

Teper, G. L. (1969). *Aircraft stability and control data.* Hawthorne, CA: Systems Technology, Inc., STI Technical Report 176-1.